ONCOIMMUNOLOGY
2026, VOL. 15, NO. 1, 2642458
https://doi.org/10.1080/2162402X.2026.2642458

Taylor & Francis
Taylor & Francis Group

RESEARCH ARTICLE

OPEN ACCESS Check for updates

Contrasting functions of CD73 and adenosine in CD8+ T-cell exhaustion during antitumor immunity

Juan Saavedra-Almarza[a,1], Solange Gouët[a,1], Felipe Malgue[a], Catalina Bascuñan[a], Andrés Hernández-Oliveras[b,c], Joaquín De la Rosa[a], Javiera Reyes-Alvarez[b], Camilo Villaman[b], José Corrales-Bermúdez[a], Justine Castañeda[d], Moira García-Gómez[a], Alberto J.M. Martin[b,e], Álvaro Lladser[b,f], Mario Rosemblatt[a,b,f], María Rosa Bono[a,b] and Daniela Sauma[a,b]

[a]Departamento de Biología, Facultad de Ciencias, Universidad de Chile, Santiago, Chile; [b]Centro Ciencia & Vida, Fundación Ciencia & Vida, Santiago, Chile; [c]Fundación Arturo López Pérez OECI Cancer Center, Laboratorio de Medicina Traslacional, Centro de Investigación e Innovación en Cáncer, Santiago, Chile; [d]Escuela de Postgrado, Facultad de Medicina, Universidad de Chile, Santiago, Chile; [e]Facultad de Ingeniería, Universidad San Sebastián, Santiago, Chile; [f]Facultad de Medicina, Universidad San Sebastián, Santiago, Chile

ABSTRACT

T-cell exhaustion is a state of functional decline in T cells, driven by chronic antigen exposure and inhibitory signals within the tumor microenvironment. Exhausted CD8+ T cells (Tex) derive from precursor exhausted T cells (Tpex), a self-renewing population responsible for the proliferative burst in anti-PD-1 therapies. Exhausted T cells are exposed to adenosine in the tumor, yet the role of the CD73/adenosine axis and Tpex/Tex differentiation remains unclear. Using an *in vitro* model for CD8+ T-cell exhaustion, we found that CD73 expression increased during Tpex formation and that its expression was negatively correlated with Tex generation. CD73-deficient OT-I cells (OT-I/CD73KO) showed impaired activation and reduced progression to Tex. Moreover, we demonstrated that CD73 promotes transcriptional expression of the adenosine receptor A2A (A2AR). RNA-seq analysis of exhausted OT-I/CD73KO cells revealed a more stem-like transcriptomic profile and enrichment in genes associated with the immune response compared to their OT-I counterparts. *In vivo*, the cotransfer of naïve OT-I/CD73KO and OT-I antigen-specific CD8$^+$ T cells into tumor-bearing mice resulted in increased Tpex frequency and numbers among OT-I/CD73KO cells in tumors. Conversely, *in vitro* exhaustion in the presence of A2AR agonists decreased Tex frequency and activation/exhaustion markers, while increasing CD73 and CD62L, which are markers associated with stemness. Supporting this, A2AR blockade with SYN115 in tumor-bearing mice reduced Tpex markers and increased Tex differentiation. Altogether, our data suggest that CD73 promotes Tpex-to-Tex differentiation, whereas adenosine A2AR signaling supports Tpex maintenance in the tumor microenvironment.

ARTICLE HISTORY
Received 22 November 2025
Revised 4 February 2026
Accepted 24 February 2026

KEYWORDS
Exhausted CD8+ T cells; Ecto-5′; NT; CD73; Adenosine; A2AR signaling; melanoma

Introduction

T-cell exhaustion is characterized as a progressive functional decline in T-cell function, driven by chronic antigen exposure and inhibitory signals within the tumor microenvironment. During exhaustion, CD8+ T cells acquire a transcriptional and epigenetic program regulated by the transcription factor TOX, which promotes their survival under sustained activation while reducing their effector potential.[1-3] Although this adaptation protects tissues from prolonged T-cell responses, it often fails to control disease progression.

Recent studies have identified a precursor population of exhausted cells (Tpex) that is crucial for the efficacy of checkpoint inhibitors[4-6] and is responsible for the proliferative burst following PD-1 blockade.[4-9] Characterized by their self-renewal capacity and expression of stem-like markers (e.g., TCF1), Tpex cells

CONTACT Daniela Sauma dsauma@uchile.cl Departamento de Biología, Facultad de Ciencias, Universidad de Chile, Las Palmeras 3425, Ñuñoa, Santiago, Chile; María Rosa Bono mrbono@uchile.cl Departamento de Biología, Facultad de Ciencias, Universidad de Chile, Las Palmeras 3425, Ñuñoa, Santiago, Chile
[1]These authors contributed equally.

Supplemental data for this article can be accessed online at https://doi.org/10.1080/2162402X.2026.2642458.

also express molecules linked to exhaustion (e.g., TOX, PD-1, LAG-3) but lack terminal exhaustion markers like TIM3, 2B4, and CD39.[1,4-6,10-12] Understanding the factors that drive Tpex differentiation into terminally exhausted (Tex) cells is key to improving immunotherapy outcomes.

Adenosine, an immunosuppressive nucleoside that accumulates within the tumor microenvironment,[13] signals through the A2A receptor (A2AR), reducing cytokine production, cytotoxicity, and T-cell proliferation.[14] Adenosine is mainly produced through ATP hydrolysis, mediated by CD39 and CD73 ectonucleotidases, which are expressed by tumor and immune cells.[14,15] While CD39 in CD8+ T cells is linked to terminal exhaustion,[11] CD73 is associated with less differentiated, stem-like cells[15] and Tpex cells.[1,16]

The immunosuppressive effect of adenosine has positioned it as a therapeutic target, with strategies often combining CD73 or A2AR blockade with PD-1 inhibition.[17,18] Indeed, some studies have shown that pharmacological blockade of CD73 or A2AR synergizes with PD-1 blockade in mice.[19-21] However, evidence suggests that complete A2AR deficiency can impair T-cell maintenance in a melanoma model,[22] and we have shown that an A2AR antagonist reduces stem-like properties in CD8+ T cells.[23] Notably, A2AR is expressed by exhausted CD8+ T cells, including Tpex,[24-26] highlighting the need to refine A2AR-targeted therapies.

CD73 may influence Tpex differentiation through mechanisms beyond adenosine production, potentially acting as a costimulatory molecule.[27-35] CD73-expressing T cells proliferate under low concentrations of PMA that are otherwise insufficient to induce proliferation in CD73-negative T cells.[33] Additionally, costimulation with anti-CD73 and anti-CD3 antibodies enhances T-cell proliferation, surpassing anti-CD3/CD28 stimulation.[29] Data from our laboratory suggest that CD73 restricts the effector program of CD8+ T cells, as evidenced by OT-I/CD73KO cells more efficiently controlling B16.OVA tumor growth and expressing lower exhaustion markers compared to OT-I cells.[36] Additionally, CD73 blockade in a murine carcinoma model reversed CD8+ T-cell exhaustion.[37] Since CD73 is expressed in Tpex, CD73 may play a key role in the differentiation of Tpex to Tex cells as a costimulatory molecule.

This study employs pharmacological and genetic approaches to investigate how adenosine signaling through A2AR and CD73 expression shapes CD8+ T-cell exhaustion *in vitro* and *in vivo* in a murine melanoma model. Our findings suggest that CD73 and A2AR contribute differently, but not necessarily in the same direction, to exhaustion dynamics, underscoring that interventions targeting distinct nodes of the CD73–adenosine pathway can have qualitatively different and context-dependent immunological consequences.

Materials and methods

Animals

C57BL/6, B6.SJL-*Ptprc*^{a}*Pepc*^{b}/BoyJ (CD45.1^{+}), B6.129S1-*Nt5e*^{tm1Lft}/J (CD73KO), B6;129-Adora2a^{tm1Dyj}/J (A2AR$^{fl/fl}$), C57BL/6-Tg(Cd8a-cre)1Itan/J (CD8-cre) (provided by Dr. Carolina Prado, Fundación Ciencia & Vida), and C57BL/6-Tg(TcraTcrb)1100Mjb/J (OT-I) were purchased from Jackson Laboratories. The OTI/CD73KO mice were generated by crossing OT-I and CD73KO mice and then backcrossing the progeny with CD73KO mice (OT-I mice served as controls). The OT-I A2AR conditional knockout (A2ARKO) mice were generated by crossing OT-I A2AR$^{fl/fl}$ mice with CD8-cre A2AR$^{fl/fl}$ mice (OT-I A2AR$^{fl/fl}$ mice were used as controls). All the mice were maintained in the animal facility of Fundación Ciencia & Vida at 26–28 °C, with 12-h light/dark cycles, with water and food *ad libitum*. The experiments were conducted with animals between 6 and 12 weeks old. Euthanasia was performed through gradual CO_2 inhalation and subsequent cervical dislocation. All experiments adhered to the ARRIVE guidelines and were conducted in accordance with the standards required by the Institutional Animal Care and Use Committee (CICUA) of Universidad de Chile (Protocol 2211-FCS-UCH).

Cell line and tumor growth

The B16.OVA cells were provided by Dr. Randolph Noelle (Dartmouth College) and cultured in RPMI +10% FBS (Sigma-Aldrich) and 55 µM β-mercaptoethanol (Gibco). The cells were maintained at 37 °C in a 5% CO_2 incubator and were routinely analyzed for mycoplasma contamination. For the tumor growth

experiments, 5×10^5 B16.OVA cells were injected intradermally into the right flank of anesthetized mice. When the tumors became palpable, their size was measured daily using a caliper.

In vitro exhaustion protocol

To obtain exhausted CD8+ T cells *in vitro*, we adapted a previously published protocol.[38] Briefly, total or naïve CD8+ T lymphocytes were magnetically isolated from the spleen of OT-I mice using the MojoSort Mouse CD8 T Cell Isolation Kit (cat: 480035, Biolegend) or the EasySep Mouse Naïve CD8+ T Cell Isolation Kit (cat: 19858, STEMCELL Technologies). The cells were cultured at 5×10^5 cells/mL in an exhaustion medium containing RPMI+10% FBS, 10 mM Hepes (cat: 15630-080, Gibco), 1 mM sodium pyruvate (cat: 11360-070, Gibco), 1% v/v nonessential amino acids (cat: 11140-050, Gibco), 55 µM β-mercaptoethanol, recombinant mouse IL-7 (cat: 577804, Biolegend) and recombinant mouse IL-15 (both at 5 ng/mL, cat: 566302, Biolegend) to generate Tpex or IL-2 (cat: 575406, Biolegend) and IL-12 (both at 10 ng/ml, cat: 577006, Biolegend) to generate Tex. For 5 d, 10 ng of SIINFEKL peptide (GenScript) was added daily. After 48 h, the cells were counted, resuspended in fresh exhaustion medium at 5×10^5 cells/mL, and transferred to a 24-well plate. On day 5, the cells were harvested and counted by FACS. As a control for acute T-cell activation, OT-I lymphocytes were activated with 10 ng of SIINFEKL peptide only on the first day for 48 h. After washing, the cells were maintained in exhaustion medium until they were analyzed.

To test the effect of adenosine on exhaustion, we added the nonhydrolysable analog of adenosine, NECA, at 1–10 µM (cat: E2387, Sigma-Aldrich), the A2AR-specific agonist CGS-21680 at 1–10 µM (cat: C141, Sigma-Aldrich), or DMSO as a vehicle control. To test the effect of CD73's enzymatic activity on exhaustion, we used the CD73 inhibitor APCP (cat: M3763, Sigma-Aldrich) at 50 µM or water as a vehicle control.

Preparation of cellular suspensions

The spleen was removed and perfused with RPMI+10% FBS, followed by centrifugation and resuspension in RBC lysis buffer (cat: 420302, BioLegend). After washing, the cells were resuspended in RPMI+10% FBS. Draining and non-draining inguinal lymph nodes were also harvested, placed in RPMI+10% FBS, and mechanically disrupted, with the resulting cell suspension filtered through a 70 µm cell strainer.

Tumors were cut into small fragments, and digested in HBSS (cat: 14185-052, Gibco) +5% FBS, DNase I at 50 µg/mL (cat: 11284932001, Roche), and collagenase D at 1 mg/mL (cat: 11088858001, Roche) using a gentleMACS dissociator (Miltenyi Biotec). The resulting cell suspension was filtered through a 70 µm cell strainer, then centrifuged and resuspended in RBC lysis buffer. Finally, the cells were washed and resuspended in HBSS+5% FBS.

Flow cytometry

Details of the antibodies used for cell staining are shown in Table 1. Nonspecific antibody binding was blocked using CD16/CD32 FcBlock (Biolegend). The Fixable Near IR Viability dye 780 (cat: L34993, Invitrogen) was used to exclude dead cells. Cells were incubated with the antibody mixture for 20 min at 4 °C, washed, and resuspended in PBS+2% FBS for FACS analysis.

For intracellular staining, after surface staining and washing, the cells were permeabilized and fixed using the FOXP3 transcription factor set (cat: 00-5523-00, eBioscience) according to the manufacturer's protocol.

t-SNE analysis was performed using a two-step concatenation strategy. First, endogenous $CD8^+$ T cells from tumor samples (control group) were concatenated into a single dataset, and endogenous $CD8^+$ T cells from tumors of mice treated with SYN115 were concatenated into a separate dataset. Subsequently, an equal number of $CD8^+$ T cells was randomly selected from each concatenated dataset, and these cells were reconcatenated to generate the final dataset used for t-SNE analysis.

Sample acquisition was performed using a BD FACSCanto II flow cytometer, a BD FACSAria III cell sorter, or a Cytek AURORA spectral cytometer. For FACS analysis, we used FlowJo version 10.4 software

Table 1. Flow cytometry antibodies.

Target	Clone	Fluorophore	Catalog number	Supplier
2B4	m2B4 (B6)458.1	PE-Cy7	133511	Biolegend
CD25	PC61.5	PE	12-0251-82	eBioscience
CD25	PC61	PerCP-Cy5.5	102030	Biolegend
CD3	17A2	APC	100236	Biolegend
CD3	17A2	BV711	100241	Biolegend
CD3	17A2	FITC	100204	Biolegend
CD39	Y23-1185	BV421	567105	BD bioscience
CD39	Duha59	PE/Dazzle594	143812	Biolegend
CD44	IM7	APC	103012	Biolegend
CD44	IM7	PerCP-Cy5.5	103031	Biolegend
CD45	30-F11	PE/Dazzle594	103145	Biolegend
CD45.1	A20	Alexa Fluor 700	110723	Biolegend
CD45.1	A20	PE-Cy7	110729	Biolegend
CD45.1	A20	PerCP-Cy5.5	110730	Biolegend
CD45.2	104	APC	109814	Biolegend
CD45.2	104	BV510	109838	Biolegend
CD45.2	104	PerCP-Cy5.5	109828	Biolegend
CD62L	MEL-14	BV570	104433	Biolegend
CD62L	MEL-14	BV785	104440	Biolegend
CD62L	MEL-14	PE	12-0621-83	eBioscience
CD62L	MEL-14	Pe-Cy7	104418	Biolegend
CD62L	MEL-14	FITC	11-0621	eBioscience
CD69	H1.2F3	BV421	104545	Biolegend
CD69	H1.2F3	PE	104508	Biolegend
CD73	TY/11.8	APC	127210	Biolegend
CD73	TY/11.8	PE-Cy7	127224	Biolegend
CD8***α***	53-6.7	APC	100712	Biolegend
CD8***α***	53-6.7	BV650	100742	Biolegend
CD8***α***	53-6.7	PE-Cy7	100722	Biolegend
IFN***γ***	XMG1.2	APC	505810	Biolegend
IFN***γ***	XMG1.2	FITC	11-7311-82	eBioscience
KLRG1	2F1/KLRG1	APC	138412	Biolegend
KLRG1	2F1/KLRG1	PE/FIRE640	138439	Biolegend
KLRG1	2F1/KLRG1	BV605	138419	Biolegend
LAG-3	C9B7W	PE-Cy7	125225	Biolegend
LAG-3	C9B7W	PerCP-Cy5.5	125212	Biolegend
LY108	330-AJ	APC	134609	Biolegend
LY108	330-AJ	Pacific Blue	134608	Biolegend
PD-1	29F.1A12	BV605	135220	Biolegend
PD-1	RMP1-30	PerCP-Cy5.5	109120	Biolegend
TCF1	C63D9	Alexa Fluor 488	6444S	Cell Signaling
TIGIT	VSIG9	BV421	142111	Biolegend
TIM-3	RMT3-23	BV785	119725	Biolegend
TIM-3	RMT3-23	PE-Cy7	119715	Biolegend
TNF***α***	MP6-XT22	BV421	506328	Biolegend
TNF***α***	MP6-XT22	FITC	506304	Biolegend
TOX	REA473	APC	130-118-335	Miltenyi Biotec
TOX	REA473	PE	130-120-716	Miltenyi Biotec
V***α***2	B20.1	PE	127808	Biolegend
V***α***2	B20.1	PE	12-5812-82	eBioscience
Vβ5.1, 5.2	MR9-4	FITC	11-5796-82	eBioscience
Vβ5.1, 5.2	MR9-4	FITC	139514	Biolegend

for macOS. For the t-SNE analyzes, R (version 4.2.2) and RStudio (version 2022.12.0+353) were used, along with an R script, and clustering was performed through DBSCAN.

Intracellular cytokine detection

Exhausted OT-I cells were restimulated by adding 10 µg of SIINFEKL peptide and 1 µL of Golgi Plug (cat: 555029, BD Biosciences) and incubated for 6 h at 37 °C and 5% CO_2. Subsequently, the cells were washed and stained with a cocktail of surface antibodies, then fixed and permeabilized before being stained with intracellular antibodies for FACS analysis.

RNA Extraction

RNA extraction was performed using the E.Z.N.A Total RNA Kit (cat: R6834-02CH, Omega Bio-tek), following the manufacturer's instructions. The resulting RNA was quantified using Qubit (Invitrogen).

RNAseq

To obtain RNA from exhausted OT-I and OT-I/CD73KO cells and perform RNA-seq, we removed dead cells from the samples by cell sorting using propidium iodide. RNAseq was performed at the Genomics and Bioinformatics Unit of the University of Santiago de Chile, creating the libraries and sequencing using the Illumina Nextseq500 platform. For public datasets, we downloaded RNA-seq data of CD8+ T cells derived from breast cancer model E0771 treated with a TY/23 antibody (anti-CD73), from Gene Expression Omnibus (accession code: GSE190603, Chen et al., 2024). Raw sequencing reads in FASTQ format were subjected to quality control using FastQC (v0.11.9) and Fastp (v1.0.1) and TrimGalore! (v 0.6.10) for adapter removal, quality trimming, and filtering of low-quality reads. Cleaned reads were aligned to the *Mus musculus* reference genome (GRCm38/mm10) using HISAT2 (v2.2.1) with default parameters. Gene-level quantification was performed with featureCounts (v2.1.1), using GENCODE comprehensive gene annotation (release M30). The resulting count matrix was imported into R (v4.2.2) for downstream analysis using DESeq2 (v1.38.3). Genes with fewer than 50 total counts across all samples were excluded to minimize noise from lowly expressed genes. Read counts were normalized using the variance-stabilizing transformation (VST) method, as implemented in DESeq2. Batch effects were corrected by including batch as a covariate in the DESeq2 design formula and further refined on the VST-transformed matrix using limma (v3.54.2). Differential expression analysis was conducted under a negative binomial generalized linear model with Wald's test for pairwise comparisons. Genes were considered differentially expressed (DEG) when the Benjamini–Hochberg adjusted *p*-value (FDR) was <0.05. Normalized and batch-corrected expression data were analyzed using the Gene Set Enrichment Analysis (GSEA) software (Broad Institute, v4.3.3). Analyzes were performed against the Hallmark (mouse 2024) gene sets from MSigDB. In addition, custom, manually curated gene signatures were included to capture specific pathways (supplementary file 1). The normalized enrichment score (NES) was computed for each gene set. A gene set was considered significantly enriched at FDR < 0.05. The top 10 enriched hallmark pathways were selected for comparative analysis. Fastq files and raw count data generated from this study are available at the Gene Expression Omnibus accession code GSE298159.

Real-time PCR

RNA from OT-I and OT-I/CD73KO cells obtained from the *in vitro* exhaustion protocol was used to generate cDNA using the Promega ImProm-II Reverse Transcriptase kit, following the manufacturer's instructions. The cDNA was mixed with primers at concentrations of 200 nM (adora3) and 400 nM (adora2a and adora2b), Brilliant II SYBR Green qPCR Master Mix (cat: 600828, Agilent Technologies), and nuclease-free water. The sequences of the primers used are shown in Table 2. The reaction was performed using a Bio-Rad CFX Connect thermal cycler and Bio-Rad CFX Maestro software. Relative expression was calculated using the Pfaffl method.

Adoptive transfer experiments

To purify naïve OT-I ($CD45.1^+CD45.2^+$) and OT-I/CD73KO ($CD45.2^+$) cells, spleen samples were enriched for total CD8+ T cells by immunomagnetic separation, and then sorted as CD44low/CD62L+/CD8+. OT-I and OT-I/CD73KO cells were mixed in a 1:1 ratio, centrifuged, and injected intravenously (1.2×10^6 cells/mouse) into tumor-bearing mice. To determine the CD73KO/WT ratio, the frequency of the respective cells in the indicated organ was compared with the frequency of these cells in the input.

Table 2. Real-time PCR primers.

Gene	Forward primer 5′ → 3′	Reverse primer 3′ → 5′
adora2a	CAC GCA GAG TTC CAT CTT CA	ATG GGT ACC ACG TCC TCA AA
adora2b	GCG AGA GGG ATC ATT GCT G	CAG GAA CGG AGT CAA TCC AA
adora3	ATA CCA GAT GTC GCA ATG TGC	GCA GGC GTA GAC AAT AGG GTT
Hprt	CTCCTCAGACCGCTTTTTGC	TAACCTGGTTCATCATCGCTAATC

SYN115 administration

C57BL/6 mice with a palpable B16.OVA tumor were injected intraperitoneally (i.p.) daily for 7 d with 3 mg/kg of SYN115 (cat: HY-10995, MedChemExpress). As a vehicle control, we used 10% DMSO + 90% corn oil (cat: C8267-500ML, Sigma-Aldrich). After the last dose, the tumor, draining node, and spleen were analyzed by FACS.

Statistical analysis

The statistical analysis was performed using GraphPad Prism software. Data normality was verified using the Shapiro–Wilk test or the D'Agostino–Pearson test. Additionally, the ROUT (Robust Regression and Outlier Removal) method was employed to identify and remove outliers. To compare two paired experimental groups with a single variable, a paired t-test was performed when the data had a normal distribution, and a Wilcoxon matched-pairs signed-rank test if the distribution was not normal. To compare two unpaired experimental groups with a single variable, an unpaired t-test with Welch's correction was used for normally distributed data, and a Mann–Whitney test was used for non-normal data distribution. To compare tumor growth curves, a two-way ANOVA with Bonferroni correction was used. To compare more than two unpaired groups of data with each other or with a control group with a single variable, a one-way ANOVA with Bonferroni correction was used. When the data were paired in the same case, a one-way repeated measures ANOVA with Bonferroni correction was used. In cases where data were normalized with respect to a control or input and compared with a theoretical value, a one-sample t-test was used for normally distributed data, or a one-sample Wilcoxon test was used for non-normally distributed data. Values of $p \leq 0.05$ were considered statistically significant, with * = $p \leq 0.05$, ** = $p \leq 0.01$, *** = $p \leq 0.001$, and **** = $p \leq 0.0001$.

Results

In vitro chronic stimulation generates exhausted cells resembling Tpex and Tex

To investigate CD73 dynamics during Tpex/Tex differentiation, we used a previously described protocol to induce exhaustion in OT-I cells.[38] We activated total OT-I lymphocytes for 5 d with the SIINFEKL peptide in the presence of IL-7/IL-15 (chronic stimulation, Figure 1A and Figure S1A). As a control, OT-I cells were activated with a single dose of SIINFEKL peptide for 48 h (acute stimulation, Figure 1A). Under chronic stimulation, we observed the generation of two populations with different levels of PD-1 and TIM3 expression, resembling Tpex (PD-1+TIM3-) and Tex cells (PD-1+TIM3+). Notably, only 10–20% of the cells expressed TIM3; thus, this protocol primarily generates exhausted cells with a Tpex phenotype (Figure 1B).

Compared to acute stimulation, chronic stimulation induced higher expression of activation markers (CD69, CD25) and recapitulated several features of exhaustion, such as the upregulation of TOX and inhibitory receptors (PD-1, TIM3, CD39, LAG-3, TIGIT, and 2B4), the reduction in the expression of stemness markers (TCF1, LY108, CD62L), and decreased effector function, as indicated by lower IFNγ and TNFα production (Figure 1C and Figure S2).

Similar to Tpex populations, PD-1+TIM3- cells from the chronically stimulated cells expressed molecules associated with exhaustion such as TOX and LAG-3, were more enriched in cells with TCF1 high expression and had a lower capacity of IFNγ and TNFα production than PD-1+TIM3+ cells (Figure 1D). Moreover, PD-1+TIM3+ cells resembled Tex as they expressed higher levels of PD-1, were more enriched in CD39+ cells, and had higher cytokine production than PD-1+TIM3- cells (Figure 1D).

Furthermore, when cultured in the presence of IL-2/IL-12 to promote terminal exhaustion, sorted PD-1+TIM3- (Tpex) cells gave rise to PD-1+TIM3+ cells, whereas when cultured with IL-7/IL-15, most cells retained a Tpex phenotype. In contrast, sorted PD-1+TIM3+ cells remained as Tex cells (Figure S3). Importantly, following adoptive transfer to B16.OVA tumor-bearing mice, PD-1+TIM3- cells persisted as Tpex and gave rise to PD-1+TIM3+ cells in the tumor niche at 3, 5 and 8 d after transfer (Figure 1E–G), indicating that *in vitro*-generated PD-1+TIM3- lymphocytes exhibit phenotypic and functional characteristics akin to Tpex.

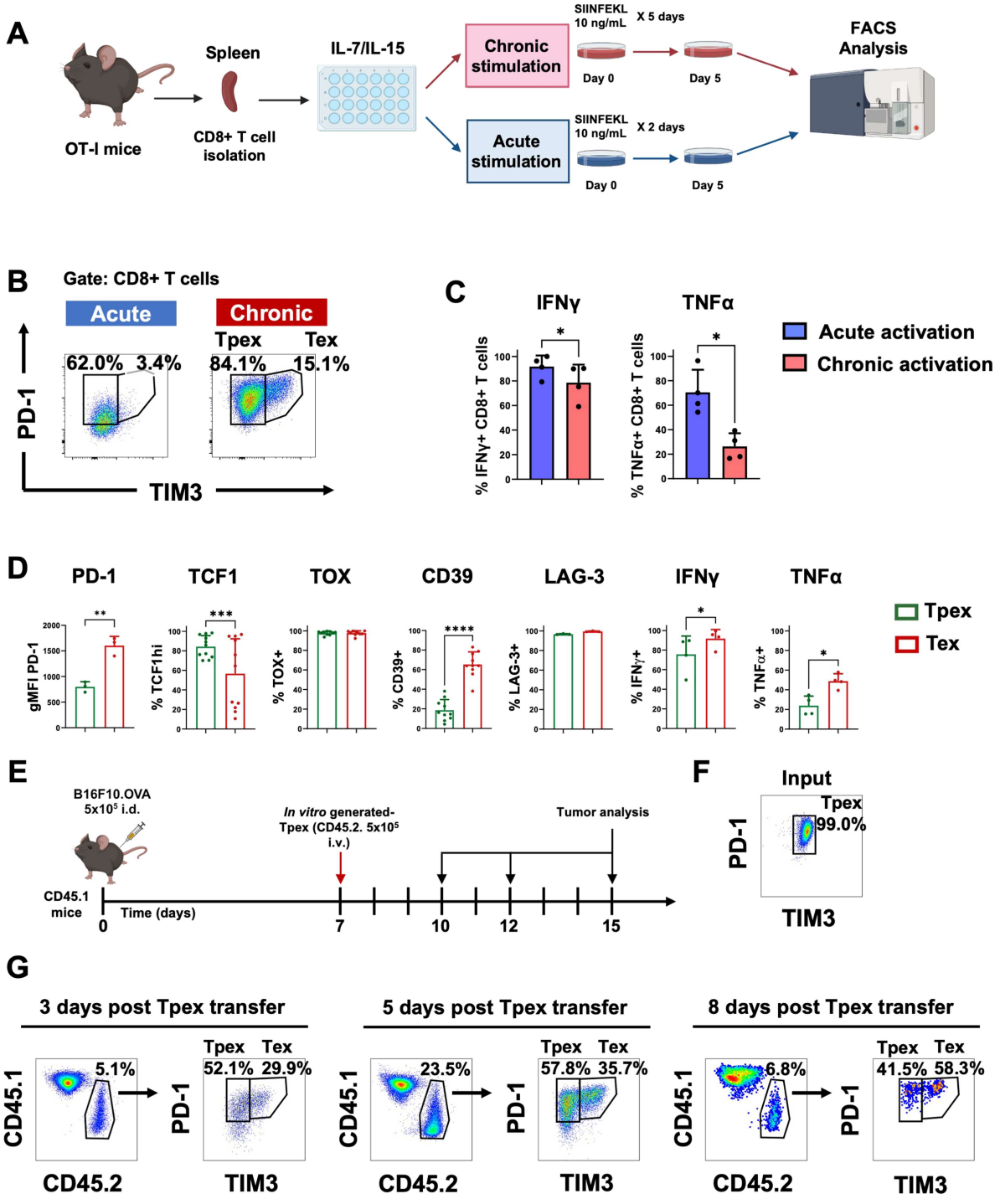

Figure 1. *In vitro*-generated exhausted CD8+ T cells are *bona fide* Tpex cells. OT-I cells were activated for 5 or 7 d (chronic activation) or for 2 d (acute activation) with the SIINFEKL peptide in the presence of IL-7 and IL-15 to generate exhausted cells and then analyzed to assess their phenotype and function. (A) Schematic overview of the protocol used to generate exhausted OT-I cells. (B) Representative dot plot of PD-1 and TIM3 expression on CD8+ T cells following acute or chronic stimulation of OT-I cells. Gates in the chronic condition depict the frequency of Tpex (PD-1+TIM3–) and Tex (PD-1+TIM3+) cells. (C) Bar graphs comparing the frequency of IFN-γ and TNFα-producing cells within chronic and acute stimulation. (D) Bar graphs showing the gMFI (for PD-1) and the frequency of cells expressing different markers within Tpex (green bars) and Tex (red bars) cells under chronic stimulation of OT-I cells. (E) Schematic overview showing the experimental strategy for adoptive transfer of *in vitro* generated Tpex cells (CD45.2+) into tumor-bearing mice (CD45.1+). (F) Dot plot depicting the phenotype of sorted *in vitro*-generated Tpex from OT-I/CD45.2+ before transfer. (G) Dot plots depicting the phenotype of *in vitro*-generated Tpex cells in tumor 3, 5, and 10 d after transfer into B16.OVA tumor-bearing mice ($n = 1, 3$ mice). Data are presented as mean ± SD. Each dot in the bar graphs represents an independent experiment ($n = 3–11$). p values were calculated using the Student's paired t-test. *$p \leq 0.05$, **$p \leq 0.01$, ***$p \leq 0.001$ and ****$p \leq 0.0001$.

CD73 expression during exhaustion

Next, we evaluated CD73 expression in *in vitro*-generated exhausted cells. We found a slight increase in CD73 expression on Tpex compared to Tex (Figure 2A). Notably, a negative correlation was observed between Tex frequency and the percentage of CD73+CD8+ T cells, indicating that CD73 expression is associated with Tpex-enriched cultures (Figure 2B).

Additionally, we assessed CD73 expression during Tpex differentiation. We sorted CD73$^-$ and CD73$^+$ naïve OT-I cells and cultured them under chronic stimulation to monitor CD73 expression (Figure 2C and D). CD73 expression in CD73$^-$ naïve CD8$^+$ T cells progressively increased, reaching ~99.73% by day 5 (Figure 2D). Conversely, in CD73$^+$ naïve CD8$^+$ T cells, CD73 expression decreased at day 1 and subsequently recovered, also reaching ~99.8% by day 5 (Figure 2D). These results indicate that CD73 is dynamically regulated under chronic stimulation, with both CD73$^-$ and CD73$^+$ naïve CD8$^+$ T cells converging to a predominantly CD73$^+$ state within 5 d.

Finally, we studied CD73 expression in the intratumoral Tpex (PD-1+TIM3-TCF1+TOX+), Tex (PD-1+TIM3+TCF1-TOX+) and an intermediate exhausted population (Tint, PD-1+TIM3-TCF1-TOX+) in the B16-OVA melanoma model (Figure 2E). Consistent with findings in chronic infections, Tpex cells exhibited a high CD73 expression (86.4%), while only 38% of Tex cells expressed CD73 (Figure 2E–F). These results indicate that CD73 expression increases during Tpex formation due to chronic activation but decreases as Tpex differentiate into Tex.

CD73 accelerates CD8+ T-cell exhaustion in vitro

CD73 not only produces adenosine but also acts as a costimulatory molecule in CD8+ T lymphocytes.[27-35] To investigate if CD73 has a costimulatory role in exhaustion, we analyzed the activation of sorted naïve CD73$^-$ and CD73$^+$ OT-I cells cultured under chronic stimulation (Figure 3A–C). After 2 d of stimulation, CD73+ cells exhibited greater proliferation and higher expression of activation markers, including CD69 and CD25, compared to CD73- cells (Figure 3A–B). By the end of the cultures, CD73- lymphocytes exhibited higher levels of CD69 and CD25 than did CD73+ lymphocytes, suggesting delayed activation (Figure 3C). Additionally, 31% of the CD73- population retained Granzyme B expression, while only 6.8% of CD73+ lymphocytes did, aligning with a Tpex phenotype (Figure 3C). These findings indicate that naïve CD8+ T cells can activate and differentiate without CD73, but at a slower rate than their CD73+ counterparts.

To confirm whether CD73 accelerates exhaustion during chronic activation, we compared exhaustion in CD73-deficient OT-I (OT-I/CD73KO) and wild-type OT-I lymphocytes. CD73 deficiency significantly reduced the Tex frequency compared to wild-type cells at the end of chronic stimulation (Figure 3D). Notably, this difference was not observed when CD73 enzymatic activity was inhibited with APCP (Figure S4), a pattern that is consistent with, but does not by itself prove, an enzyme activity–independent contribution of CD73 to exhaustion dynamics. Thus, CD73 enhances the activation and exhaustion of CD8+ T lymphocytes *in vitro*.

CD73KO cells display a transcriptional shift towards a stem-like state

To further investigate the contribution of CD73 to exhaustion, we analyzed the transcriptomic profile of *in vitro*-exhausted OT-I and OT-I/CD73KO cells using RNAseq. PCA analysis showed that exhausted OT-I and OT-I/CD73KO cells were transcriptionally distinct, clustering in separate regions of Principal Component 1 (PC1) (Figure 4A). Transcriptomic analysis showed differential expression of 66 genes, with 56 upregulated in the OT-I/CD73KO samples and 12 upregulated in the OT-I samples (Figure 4B). Among the upregulated genes in exhausted OT-I/CD73KO cells we found *Bcl2l11*, encoding the canonical BH3-only pro-apoptotic initiator protein BIM; *Sell*, encoding CD62L, associated with stem-like states; *Klf2*, encoding the transcription factor KLF2, which has been shown to regulate CD62L and CCR7 expression, suppress TOX and drive effector differentiation[39]; *Cd101*, encoding the glycoprotein CD101 associated with terminal exhaustion in viral infections; and several genes associated with immune signaling and interferon responses (e.g., Ifit3, Irf7, Ifi44, Usp18, Zbp1). On the other hand, among the upregulated genes in exhausted OT-I lymphocytes, we found *Batf3*, which has been linked to exhaustion[40]; and *Gzmb*, which encodes granzyme B expressed in effector and exhausted cells, but not in Tpex.

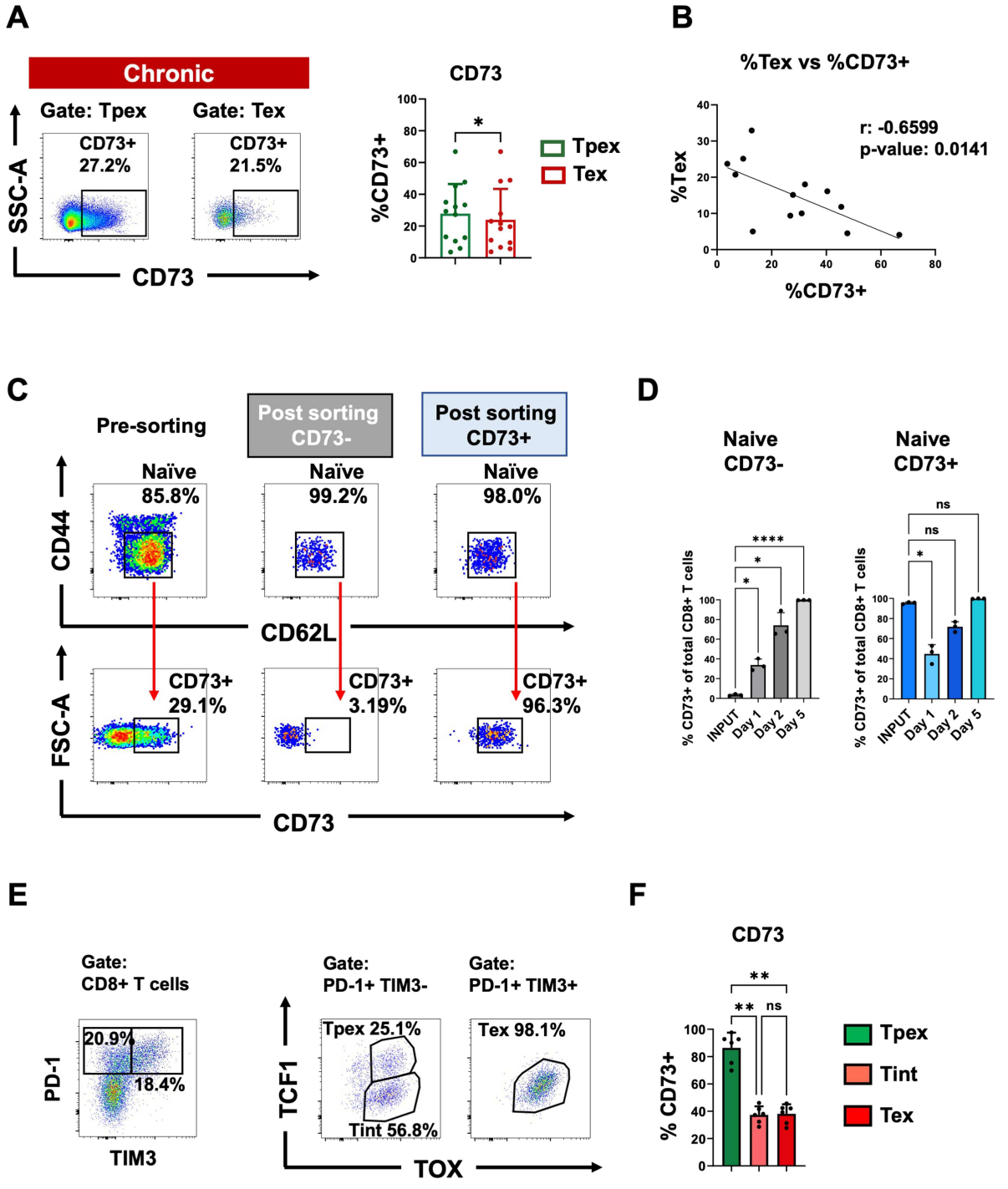

Figure 2. CD73 is expressed in the precursors of exhausted CD8+ T cells, and its expression decreases upon terminal differentiation. (A) Representative dot plot depicting the frequency of CD73+ within Tpex and Tex cells following 5 d of chronic stimulation of OT-I cells. Bar graph shows the frequency of CD73+ T cells within Tpex (green bar) and Tex (red bar) cells following 5 d of chronic stimulation. (B) Correlation between the percentage of CD73+ cells and Tex frequency at the end of the cultures following chronic stimulation of OT-I cells for 5 d. A–B, Each dot represents an independent experiment ($n = 13$). (C–D) Naïve OT-I cells were sorted based on CD73 expression and cultured for 5 d under chronic stimulation to assess the kinetics of CD73 expression. (C) Dot plots depicting the phenotype of OT-I cells before and after sorting of CD73– and CD73+ naïve populations. (D) Bar graphs show the frequency of CD73+ OT-I cells at day 0 (input) and over 1, 2, and 5 d of chronic stimulation of sorted CD73– and CD73+ naïve OT-I cells. C–D, Each dot represents an independent experiment ($n = 3$). (E) Left: Dot plot depicting PD-1 and TIM3 expression in tumor-infiltrating CD8+ T cells. Right: Dot plots depicting TCF1 and TOX expression in PD-1+ TIM3– and PD-1+TIM3+ populations of tumor-infiltrating CD8+ T cells. The gates represent the frequency of cells within Tpex, Tint, and Tex compartments. (F) Bar graph showing CD73+ CD8+ T cells within tumor-infiltrating Tpex (green bar), Tint (light red bar), and Tex (dark red bar) compartments.

(*Caption on next page*)

Data are presented as mean ± SD. E–F, Each dot in the bar graphs represents the results from one mouse (total of 6 mice). *P* values were calculated using the Wilcoxon test (A), simple linear regression (B), One-way ANOVA with Bonferroni's post-test (D and F). *$p \leq 0.05$, **$p \leq 0.01$, and ****$p \leq 0.0001$. ns not significant.

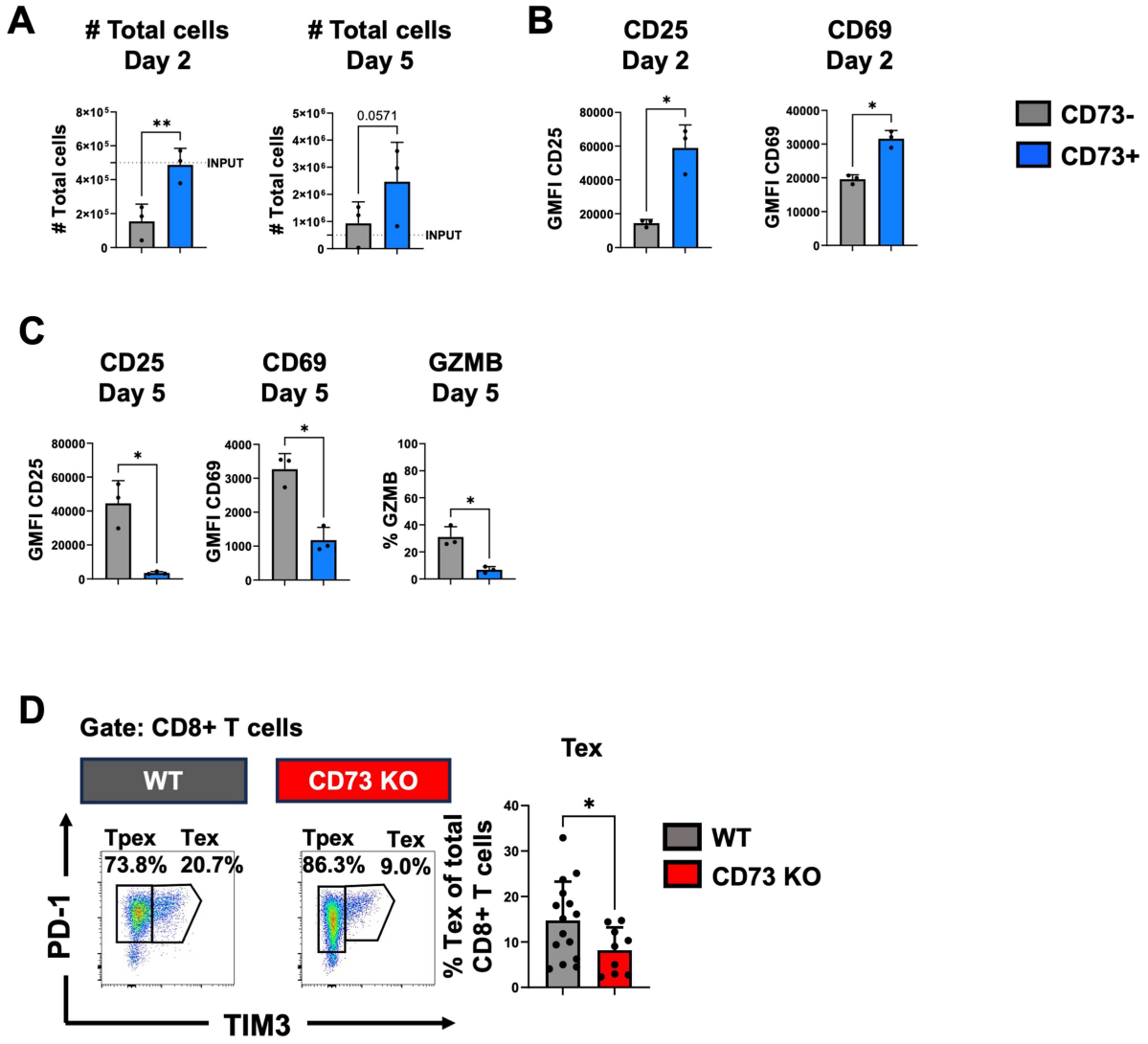

Figure 3. CD73 accelerates the exhaustion process in CD8+ T cells *in vitro*. (A) CD73- and CD73+ OT-I cells were sorted and activated with the SIINFEKL peptide and IL-7/IL-15 for 2 or 5 d. The bar graph shows the absolute numbers of total cells in the cultures following chronic activation of CD73− (gray) and CD73+ (blue) CD8+ T cells. The dotted line represents the number of cells at day 0 (input). (B) Bar graphs showing CD25 and CD69 mean fluorescence intensity on CD73− (gray bars) and CD73+ (blue bars) on OT-I cells chronically activated for 2 d. (C) Bar graphs showing mean fluorescence intensity of CD25 and CD69, and the frequency of granzyme B (GZMB) expressing cells on CD73− (gray bars) and CD73+ (blue bars) OT-I cells that were chronically activated for 5 d. A–C, each dot represents an independent experiment ($n = 3$). (D) OT-I and OT-I/CD73KO cells were chronically activated with the SIINFEKL peptide and IL-7/IL-15 for 5 d. Dot plots depict PD-1 and TIM3 expression in OT-I and OT-I/CD73KO cells following 5 d of chronic stimulation. The gates show the frequency of Tpex and Tex cells. The bar graph shows the frequency of Tex cells after 5 d of chronic activation of OT-I (gray bar) and OT-I/CD73KO (red bar) cells. Data are presented as mean ± SD. Each dot in the bar graphs represents an independent experiment ($n = 9–15$). *P* values were calculated using the Student's paired t-test (A–C) and unpaired t-test with Welch's correction (D). *$p \leq 0.05$, **$p \leq 0.01$.

While both the transcriptomic analysis of the cytotoxic profile and Granzyme B (gzmb) levels are reduced in CD73KO cells compared to WT cells (Figure 4B–D), we did not observe any differences in Granzyme B production by flow cytometry between WT and CD73KO cells (data not shown).

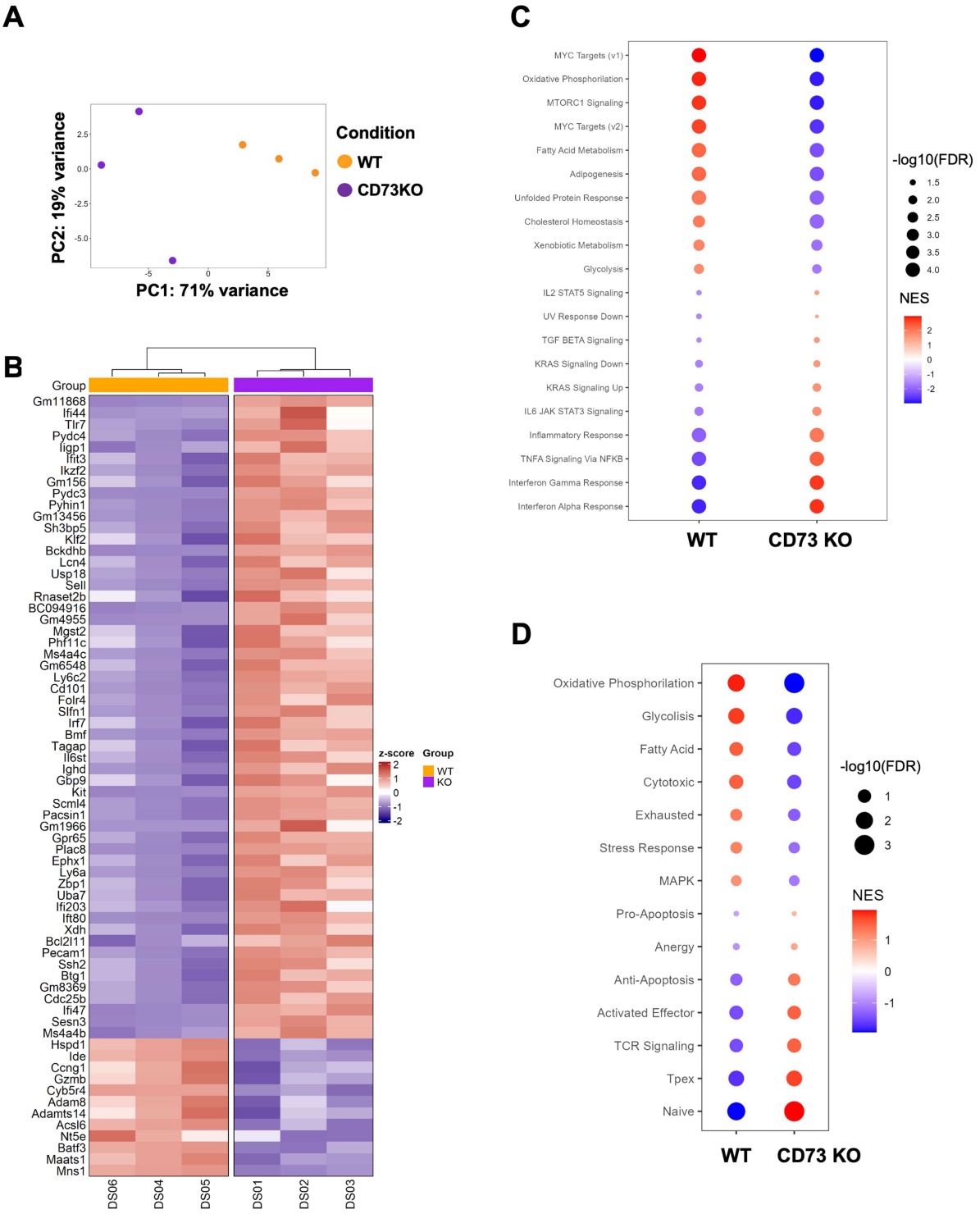

Figure 4. CD73 deficiency promotes a stem-like transcriptional profile in exhausted CD8+ T cells. OT-I and OT-I/CD73KO cells were activated for 5 d under chronic stimulation with the SIINFEKL peptide in the presence of IL-7 and IL-15 and analyzed by RNAseq. (A) PCA analysis of WT and CD73KO RNAseq samples. Each dot represents an independent experiment (WT $n = 3$, CD73KO $n = 3$). (B) Heat map showing a set of genes upregulated and downregulated in WT cells compared to CD73KO cells. (C) Gene set enrichment analysis for functional pathways was performed using the expression matrix of the data and the hallmarks of the MsigDB as a reference. (D) Gene set enrichment analysis for function-associated signatures.

To understand the functional pathways enriched in *in vitro*-exhausted OT-I and OT-I/CD73KO cells, we performed gene set enrichment analysis using the expression matrix of the data and the hallmarks of MsigDB as a reference (Figure 4C). Exhausted OT-I/CD73KO cells were enriched in functional pathways associated with pathogen defense and immunity (inflammatory response, TNF signaling via NFκB, IFNγ and IFNα response), while exhausted OT-I cells were enriched in metabolic pathways (oxidative phosphorylation, fatty acid metabolism, adipogenesis, MTORC1 signaling), unfolded protein response, and MYC targets (Figure 4C). Interestingly, constitutive MTORC1 activation promotes a terminally differentiated effector phenotype, and recent evidence suggests a role for c-MYC in promoting exhaustion.[41,42]

Next, we compared the transcriptomic profile of exhausted OT-I and OT-I/CD73KO cells with manually curated cell and function-associated signatures (Figure 4D). We found a greater similarity to a stem-like, naïve, and Tpex phenotype in OT-I/CD73KO cells compared to OT-I cells, while OT-I cells showed greater enrichment of gene expression associated with glycolysis and oxidative phosphorylation (Figure 4D). Thus, CD73-deficient CD8+ T cells display a transcriptional shift toward a more stem/naïve-like state (e.g., Klf2 and Sell) alongside a prominent type I interferon–associated program (e.g., Irf7 and multiple ISGs). Notably, they also show evidence of selective apoptotic priming – including increased Bcl2l11 (BIM) without a coordinated enrichment of broad pro- versus anti-apoptotic gene sets, consistent with priming rather than overt apoptotic execution.

We also analyzed $CD8^+$ T cells derived from the E0771 breast cancer model treated with the TY/23 anti-CD73 antibody. Principal component analysis (PCA) of two control and three anti-CD73–treated samples revealed a clear separation between control and anti-CD73 conditions along PC1 (Figure S5A). The use of anti-CD73 antibody was associated with increased expression of gene programs related to TCR signaling, co-stimulation, interferon response, exhaustion, stemness, MAPK signaling, effector function, and purinergic signaling, as well as elevated expression of the Fyn, Lck, and Havcr2 (TIM3) genes (Figure S5B–C). This suggests that CD73 may signal through Lck and Fyn to promote exhaustion in CD8+ T cells.

CD73 deficiency enhances Tpex maintenance in tumors and DLN

Given that exhausted OT-I/CD73KO lymphocytes display a stem-like transcriptomic profile, we examined how CD73 deficiency influences the maintenance and phenotype of OT-I lymphocytes *in vivo* in a melanoma model. Naïve OT-I and OT-I/CD73KO cells were cotransferred into B16.OVA tumor-bearing mice at a 1:1 ratio (Figure 5A). Following co-transfer, tumor growth at early time points showed no significant differences between the co-transferred and non-transferred control groups (Figure 5B). Seven days post-co-transfer, we analyzed CD8+ T-cell frequency and phenotype in the tumor, spleen, draining lymph nodes (DLN), and nondraining lymph nodes (LN). Co-transferred cells were more represented in the tumor and DLN, at a low frequency in the spleen, and almost absent in the LN (Figure 5C–D). Interestingly, both the DLN and the tumor exhibited a higher frequency of OT-I/CD73KO lymphocytes compared to OT-I lymphocytes. In the tumor, the absolute number of OT-I/CD73KO lymphocytes was also greater than their OT-I counterparts (Figure 5C–D).

FACS and t-SNE analysis of cotransferred CD8+ T cells revealed that both OT-I and OT-I/CD73KO cells differentiated primarily into Tpex (PD-1+TOX+TCF1+TIM3-) in both tumor and DLN (Figure 5E, Figure S6). In the tumor and DLN, OT-I/CD73KO cells differentiated slightly more into a Tpex phenotype than their OT-I counterparts (Figure 5E). We observed no significant differences between OT-I and OT-I/CD73KO Tex cells (Figure 5E).

To further study the effect of CD73 in the Tpex to Tex transition, we transferred OT-I and OT-I/CD73KO Tpex cells into B16.OVA tumor-bearing mice and followed their transition to Tex cells. As shown in Figure S7, OT-I/CD73KO Tpex cells retained their phenotype and differentiated less to Tex cells than OT-I/WT Tpex cells. Thus, the adoptive transfer experiments of OT-I/WT and OT-I/CD73KO cells suggest that CD73 deficiency reduces the acquisition of the Tex phenotype.

Adenosine via A2AR delays Tex formation in vitro

Considering that the most recognized function of CD73 is as an adenosine-producing ectoenzyme, we evaluated how adenosine signaling influences exhaustion. *In vitro*-exhausted OT-I cells primarily

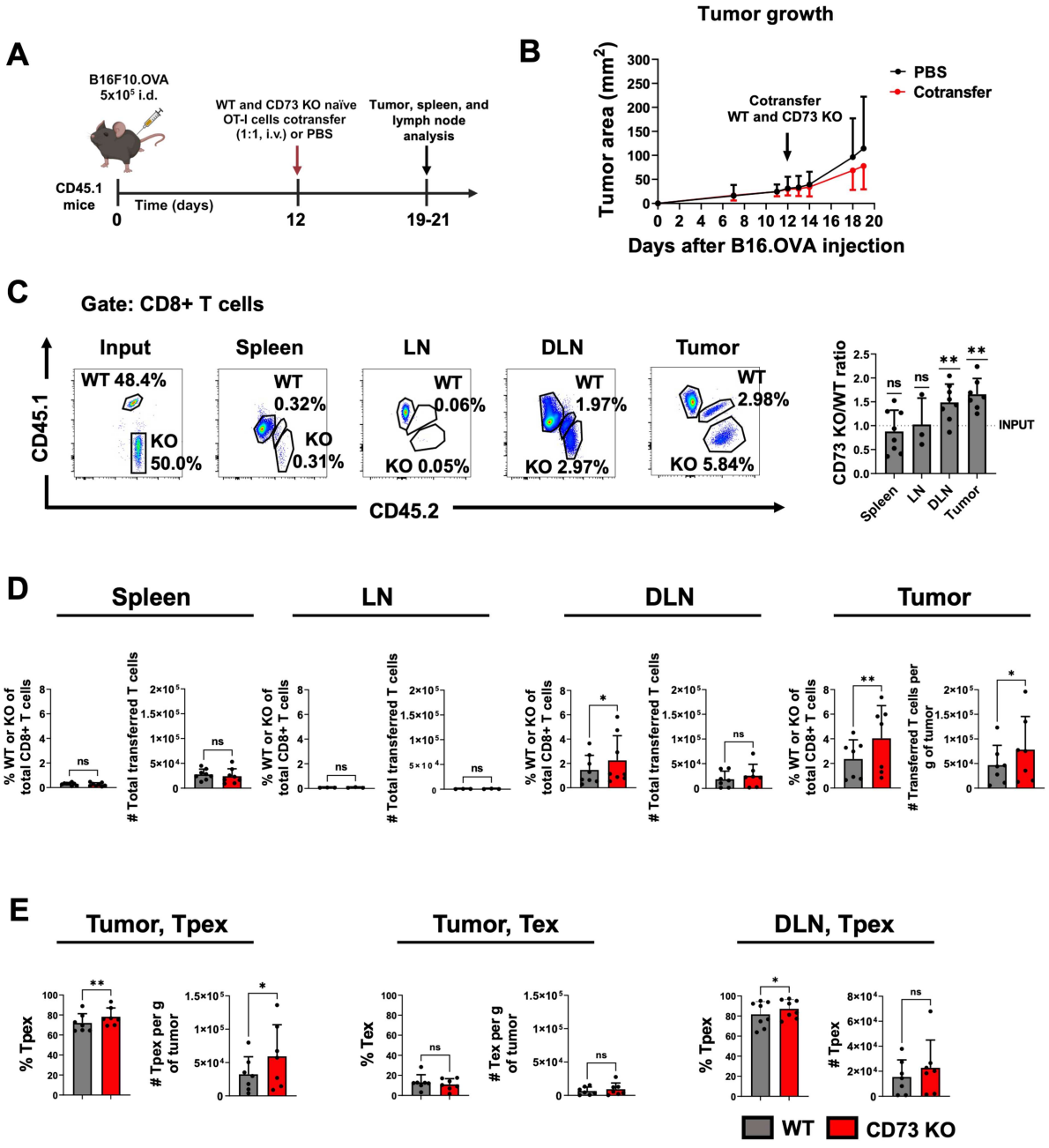

Figure 5. CD73 deficiency enhances Tpex maintenance in tumors and tumor-draining lymph nodes. Naïve OT-I and OT-I/CD73KO cells were co-injected in a 1:1 ratio into B16-OVA tumor-bearing mice. Mice were euthanized when tumors reached a size of 50–100 mm^2, and the transferred cells were analyzed by flow cytometry. (A) Schematic overview showing the experimental strategy for adoptive transfer experiments of OT-I and OT-I/CD73KO cells into tumor-bearing mice. (B) Tumor area in mice cotransferred with OT-I and OT-I/CD73KO cells (red line, 8 mice) compared to mice only injected with PBS (black line, 4 mice). (C) Dot plots depicting the frequency of OT-I (CD45.1+/CD45.2+) and OT-I/CD73KO (CD45.2) cells at the input and different tissues following transfer to CD45.1 tumor-bearing mice. Endogenous cells are distinguished as CD45.1+ cells. The gates depict the frequency of OT-I and OT-I/CD73KO transferred cells. The bar graph illustrates the ratio of OT-I/CD73KO and OT-I transferred cells within various tissues. The dotted line represents the input ratio. (D) Bar graphs showing the frequency and absolute numbers of OT-I (gray bars) and OT-I/CD73KO (red bars) cells in spleen, nondraining lymph nodes (LN), tumor-draining lymph nodes (DLN), and tumor. (E) Bar graphs showing the frequency and absolute number of Tpex and Tex from OT-I (gray bars) and OT-I/CD73KO (red bars) cells in the tumor and tumor-draining lymph node. Data are presented as mean ± SD. Each dot in the bar graphs represents one mouse. Spleen and DLN $n = 8$, LN $n = 3$, and tumor $n = 7$. *P* values were calculated using the one sample t and Wilcoxon test (C) and Student's paired t-test or the Wilcoxon test (D–E). $^*p \le 0.05$, $^{**}p \le 0.01$. ns not significant.

expressed the adenosine receptor A2AR and lacked expression of the other adenosine receptors (Figure 6A). Interestingly, *in vitro*-exhausted OT-I/CD73KO cells exhibited reduced A2AR expression relative to OT-I cells (Figure 6A).

Although our *in vitro* protocol generates preferentially Tpex cells and a low frequency of Tex cells, we could observe that the activation of A2AR with 10 μM CGS21680 further reduced the frequency of OT-I Tex cells at the end of the culture (Figure 6B). Both NECA and CGS21680 increased the frequency of CD73+ exhausted cells, and enrichment of CD62L+ cells was observed in the exhausted populations treated with CGS21680. However, TCF1 expression levels remained unaffected by either treatment (Figure 6C, Figure S8). In contrast, both NECA and CGS21680 decreased the expression of activation markers CD25 and CD44 in exhausted cells (Figure 6C, Figure S8). Interestingly, both compounds also reduced TOX expression levels (Figure 6C, Figure S8), while PD-1 expression was only decreased with specific A2AR activation using CGS21680 (Figure 6C, Figure S8).

To determine whether A2AR contributes to delaying the exhaustion process during chronic activation of CD8+ T cells, we performed cultures of OT-I/A2ARKO and OT-I control lymphocytes. In contrast to the reduction in Tex frequency observed in cultures of OT-I/CD73KO cells, the absence of A2AR expression in OT-I lymphocytes resulted in a significant increase in the frequency of Tex cells at the end of chronic stimulation, compared to OT-I control lymphocytes (Figure 6D). The specificity of CGS21680 was demonstrated in the A2ARKO cells, as this A2AR agonist did not reduce Tex whereas we observed an increase on Tex cells when cultured with NECA, suggesting that NECA may be signaling through other adenosine receptor (Figure S9).

Thus, unlike the accelerating effect of CD73 in exhaustion, adenosine via A2AR delays the *in vitro*-exhaustion of OT-I cells, reducing the frequency of Tex at the end of culture, the expression of molecules associated with exhaustion and activation, and promoting the expression of stem-like–associated molecules such as CD62L and CD73.

Systemic A2AR antagonism skews tumor-infiltrating CD8+ T cells toward a Tex phenotype

Ultimately, we aimed to investigate the role of adenosine signaling through A2AR in the exhaustion of CD8+ T cells in the context of cancer. B16.OVA tumor-bearing mice were treated with the A2AR-specific pharmacological inhibitor SYN115 (3 mg/kg) one week post-tumor injection, and the phenotype of intratumoral CD8+ T cells was subsequently analyzed by FACS (Figure 7A). No significant differences in tumor growth were observed between SYN115-treated mice and vehicle-treated mice over the period studied (Figure 7B). SYN115 treatment did not alter the frequency or total number of CD8+ T cells in the spleen, DLN, or tumor (Figure S10A).

Through dimensionality reduction analysis using t-SNE of FACS data from intratumoral CD8+ T cells from treated and untreated mice, qualitative differences in the distribution of the various CD8+ T-cell populations were observed (Figure 7C and S10B). Unlike the results of the control group, where intratumoral CD8+ T-cell populations were homogeneously distributed, treatment with SYN-115 favored the formation of CD73- Tex (Figure 7C) and showed reduced densities across the other $CD8^+$ T-cell populations, except for Tpex cells, consistent with a net shift toward a more terminally exhausted phenotype under systemic A2AR antagonism.

Next, we performed conventional FACS analysis of the frequency and phenotype of Tpex and Tex populations, as well as exhaustion markers (TOX, PD-1, and CD39), memory/stem cell markers (CD73 and TCF1), and effector cell markers (KLRG1) (Figure 7D–E and S10C) in SYN115-treated mice. Thus, whereas the frequency of Tpex did not change significantly, we observed a significant increase in the frequency of intratumoral Tex cells relative to the control group (Figure 7D). Furthermore, while treatment with SYN115 increased the frequency of intratumoral TOX+ CD8+ T cells, and those cells that express high levels of PD-1 and CD39, it reduced the frequency of CD73+ and TCF1+ cells, while it did not significantly affect the frequency of KLRG1+ effector T cells (Figure 7E and S10C).

Altogether, systemic A2AR antagonism with SYN115 was associated with increased Tex frequency and higher TOX/PD-1hi/CD39hi expression, along with reduced frequencies of $CD73^+$ and $TCF1^+$ $CD8^+$ T cells in tumors (Figure 7D–E). Because SYN115 is administered systemically and A2AR is expressed across multiple immune and non-immune compartments, these *in vivo* findings should be interpreted as the net

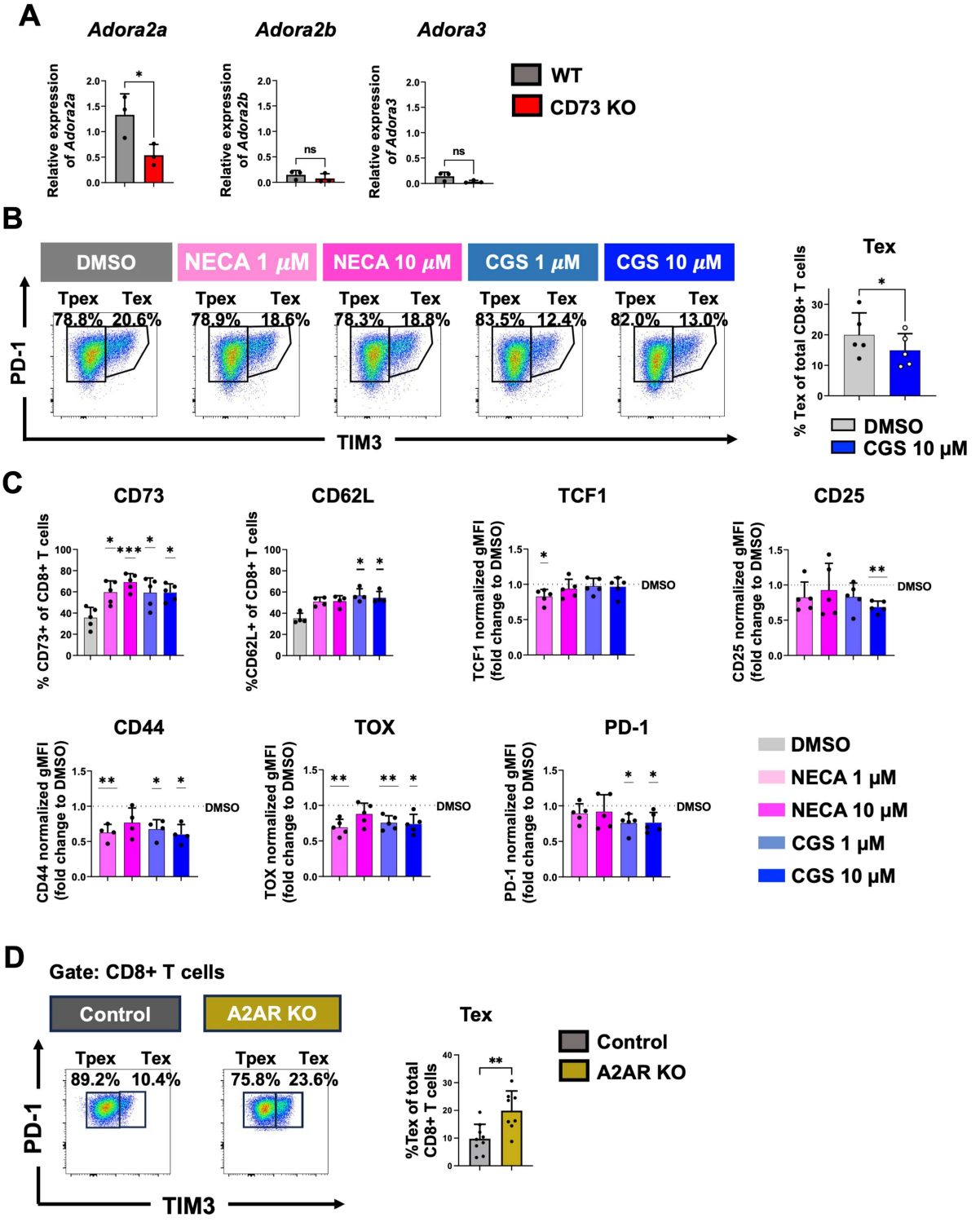

Figure 6. A2AR signaling delays Tex formation *in vitro*. (A) OT-I and OT-I/CD73KO cells were activated for 5 d under chronic stimulation with the SIINFEKL peptide in the presence of IL-7 and IL-15, and then analyzed by real-time PCR to determine adenosine receptor expression. Data were normalized with the *hprt* housekeeping gene. Each dot represents an independent experiment ($n = 3$). (B) OT-I cells were activated for 5 d with the SIINFEKL peptide (chronic stimulation) in the presence of IL-7/IL-15 and different A2AR agonists (NECA, CGS-21680) at 1 and 10 μM. DMSO was used as the vehicle control. Dot plots show PD-1 and TIM3 expression, depicting the frequency of Tpex and Tex cells under each treatment. The bar graph compares the frequency of Tex cells in cultures with CGS-21680 10 μM (blue bar) and DMSO (gray bar). (C) Bar graphs comparing the frequency of CD73+ cells and CD62L+ cells and the normalized mean fluorescence intensity of TCF1, CD25, CD44, TOX, and PD-1 under each treatment. B–C, Each dot represents an independent experiment ($n = 5$). (D) OT-I control and OT-I/A2ARKO cells were activated for 5 d with the SIINFEKL peptide (chronic activation) in the

(*Caption on next page*)

presence of IL-7/IL-15. Dot plots showing PD-1 and TIM3 expression, depicting the frequency of Tpex and Tex cells in OT-I control and OT-I/A2ARKO cells. The bar graph shows the frequency of Tex cells in OT-I control and OT-I/A2ARKO cells following 5 d of chronic stimulation. Data are presented as mean ± SD. Each dot in the bar graphs represents an independent experiment (control $n = 9$ and A2AR KO $n = 8$). *P* values were calculated using the unpaired t-test (A and D), Student's paired t-test (B) or one-way ANOVA (CD73 and CD62L) and one-sample t and Wilcoxon test (TCF1, CD25, CD44, TOX, and PD-1) (C). *$p \leq 0.05$, **$p \leq 0.01$, ***$p \leq 0.001$. ns not significant.

consequence of a system-level perturbation of A2AR signaling in the tumor microenvironment, rather than as definitive evidence of a CD8+ T cell-intrinsic mechanism.

Discussion

The adenosine-producing function of CD73, along with its expression in various tumor types, has positioned this enzyme as a promising therapeutic target in cancer treatment. Consequently, CD73-blocking antibodies are being developed to limit adenosine production, often without fully considering its expression on immune cells and nonenzymatic activities. Here, we demonstrate that CD73 may accelerate exhaustion in CD8+ T lymphocytes, an effect likely independent of its adenosine-producing capacity, and potentially linked to its costimulatory role. This finding is vital for future cancer therapies, as it highlights the need to consider the multifaceted roles of CD73 in immune regulation, ensuring that therapeutic strategies optimize T-cell function without inadvertently promoting exhaustion.

In the early stages of T-cell activation, adenosine receptor expression, particularly that of the A2A receptor (A2AR), is relatively low. Studies indicate that this expression significantly increases over days following activation.[22] It is possible to hypothesize that during this initial phase, adenosine signaling may not play a predominant role, suggesting that the catalytic activity of CD73, which converts extracellular ATP to adenosine, may not be the primary driver of T-cell responses at this time. Instead, CD73 might function more prominently as a costimulatory molecule, enhancing T-cell activation through mechanisms that are independent of its enzymatic function. This hypothesis aligns with the observation that while A2AR signaling becomes crucial later in the activation process, its initial low expression may allow other costimulatory signals to dominate T-cell responses during the critical early activation phase.

The costimulatory role of CD73 has been previously evaluated in human CD73+ and CD73- T cells, showing that cells expressing CD73 require lower concentrations of PMA for activation.[33] Our results extend this observation: OT-I CD73+ cells display characteristics of activated T cells earlier than their CD73- counterparts under the same activation conditions. Moreover, CD73 deficiency delayed differentiation into Tex cells *in vitro* and promoted a stem-like transcriptional profile akin to that of Tpex, suggesting a role of CD73 as a promoter of exhaustion.

Interestingly, the costimulatory function of CD73 on T lymphocytes can be activated with antibodies that block its enzymatic activity.[27,35] This raises concerns that therapies targeting CD73 could inadvertently enhance CD8+ T lymphocyte exhaustion through its costimulatory function. Supporting this, a study reported that blocking CD73 with an antibody in tumor-bearing mice restored some effector functions of CD8+ T cells, but also increased expression of CTLA-4 and PD-1 in CD73+ T cells.[37] Although the authors attributed this to a "resistant phenotype" to therapy, it could reflect the activation of the costimulatory function of CD73 by the antibody, thereby accelerating the exhaustion of CD8+ T cells. In addition, the analysis of RNA-seq data obtained from infiltrating CD8+ T cells from E0771-bearing mice treated with anti-CD73[43] demonstrated that the CD73 antibody (TY/23) induces lck, fyn and havcr2 (TIM3) gene expression, supporting our data that CD73 may be signaling through lck and fyn to promote exhaustion in CD8+ T cells.

CD73 expression was enriched in Tpex and was low or absent in intratumoral Tex, which, on the one hand, suggests that CD73 is a marker of Tpex and, on the other hand, could indicate that this molecule is necessary for the differentiation of Tpex into Tex. However, we have demonstrated that adenosine reduces exhaustion through A2AR. The contrast between the role of adenosine via A2AR and CD73 in exhaustion further supports the idea that the role of CD73 in this process is independent of its adenosine-producing function.

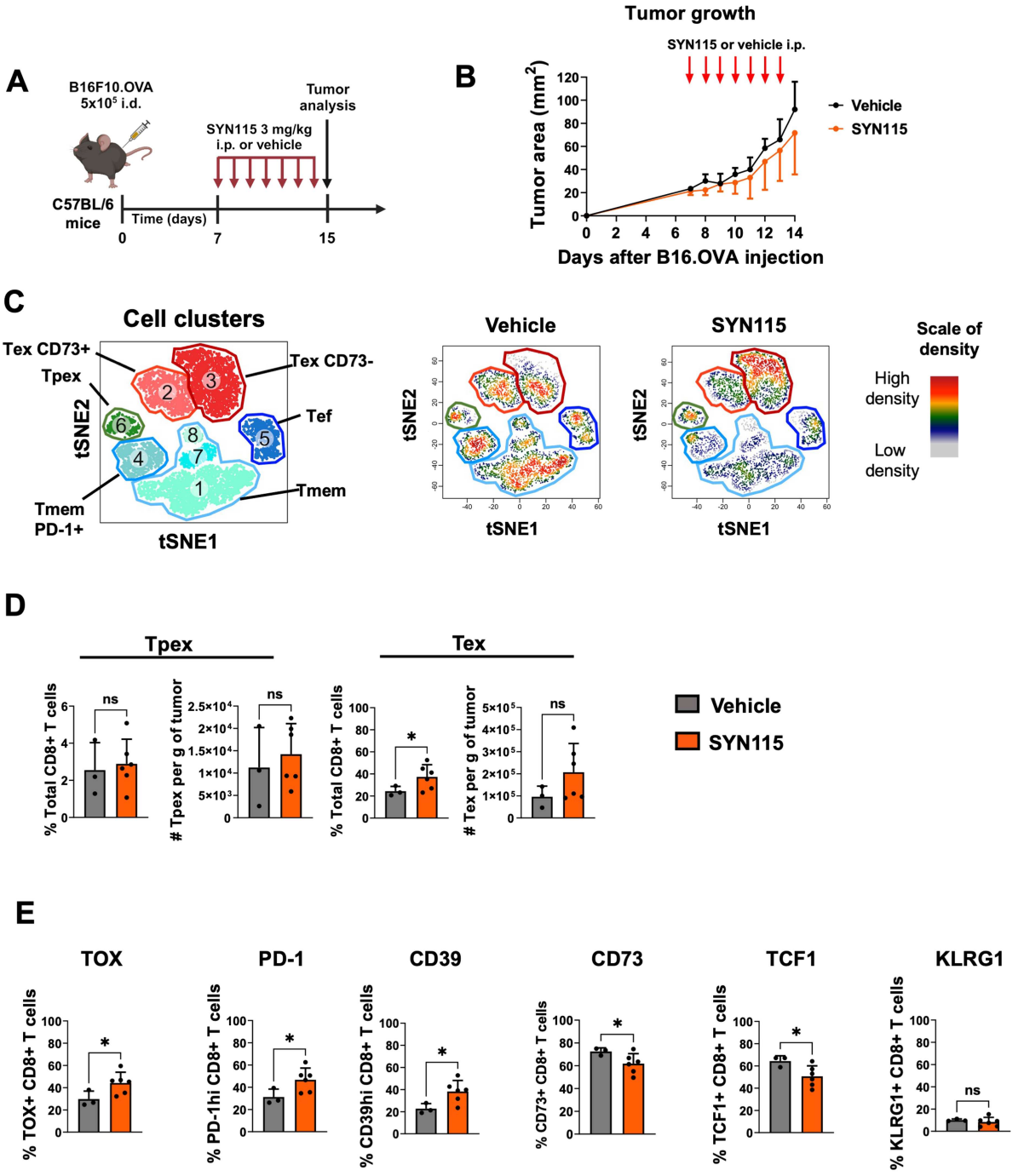

Figure 7. Systemic A2AR antagonism skews tumor-infiltrating CD8+ T cells towards a Tex phenotype. B16-OVA tumor-bearing mice were treated daily with the A2AR antagonist SYN115. Mice were euthanized when tumors reached a size of 50–100 $mm^{2,}$ and tumor-infiltrating CD8+ T cells were analyzed by flow cytometry. (A) Schematic overview showing the experimental strategy of SYN115 treatment in tumor-bearing mice. (B) Tumor area in mice injected with SYN115 (orange line, 6 mice) compared to mice only injected with vehicle control (black line, 3 mice). (C) T-Sne analysis of endogenous tumor-infiltrating CD8+ T cells showing the different clusters of exhausted and memory CD8+ T cells in control and SYN115-treated mice. (D) Bar graphs showing the frequency and number of Tpex and Tex cells per gram of tumor in SYN115-treated mice Compared to controls. (E) Bar graphs showing the frequency of TOX+, PD-1+, CD39 hi, CD73+, TCF1+, and KLRG1+ CD8+ T cells in SYN115-treated mice Compared to control. Data are presented as mean ± SD. Each dot in the bar graphs represents one mouse (vehicle $n = 3$ and SYN115-treated mice $n = 6$). *P* values were calculated using an unpaired t-test with Welch's correction. *$p \leq 0.05$. ns not significant.

Gene set enrichment analysis revealed that exhausted OT-I/CD73KO cells were enriched in pathways linked to pathogen defense and immunity, such as the inflammatory response, TNF signaling via NFκB, and IFNγ and IFNα responses, while OT-I cells showed enrichment in metabolic pathways. This suggests that CD73 deficiency shifts CD8$^+$ T cells towards a more stem/naïve-like state and enhances type I interferon responses. These insights suggest that CD73 deletion in cancer therapies could enhance T-cell responses by modulating exhaustion and promoting a more favorable immune profile.

In contrast to CD73, our results suggest that adenosine, via the A2AR, can delay terminal exhaustion and maintain stemness-associated features in CD8+ T cells. Pharmacological activation of adenosine signaling via the A2AR during *in vitro* exhaustion of OT-I cells decreased the expression of exhaustion markers, Tex frequencies, and activation while increasing the expression of CD73 and CD62L on CD8+ T cells. In agreement, A2AR genetic deletion on CD8+ T cells favored their differentiation to Tex, demonstrating a cell-intrinsic role of adenosine in restraining CD8+ T-cell differentiation.

This systemic intervention was associated with increased Tex frequency and higher TOX/PD-1hi/CD39hi expression, along with reduced CD73$^+$ and TCF1$^+$ frequencies among intratumoral CD8$^+$ T cells compared to controls. Importantly, because SYN115 is administered systemically and A2AR is expressed on multiple immune and stromal compartments, these *in vivo* effects reflect a net system-level perturbation and cannot be attributed solely to CD8$^+$ T cell-intrinsic A2AR signaling. Our CD8$^+$ T cell-intrinsic interpretation is supported primarily by genetic A2AR deletion in CD8$^+$ T cells *in vitro* and by prior work showing that CD8$^+$ T-cell A2AR deficiency compromises persistence and/or survival within tumors.[22] Together, these data support a "double-edged sword" model in which A2AR signaling can restrain differentiation programs associated with terminal exhaustion while also contributing to the maintenance of CD8$^+$ T cells in chronic antigen settings. Hence, adenosine via A2AR could play a similar role as PD-1, where its expression is not required to generate Tex, but in its absence, exhausted cells accumulate in chronic infections.[44]

It is important to recognize that the accumulation of exhausted T cells (Tex), driven by the differentiation of precursor exhausted T cells (Tpex), may serve as a biomarker of therapeutic response, particularly in the context of PD-1 blockade.[45] While terminally differentiated T cells are often viewed unfavorably, the activation and differentiation of Tpex are crucial for initiating an effective antitumor immune response. Studies have shown that robust Tpex activation can enhance tumor-specific responses, highlighting the necessity of T-cell differentiation. Thus, while Tex accumulation may indicate immune dysfunction, the differentiation process from Tpex is a fundamental component of the immune response that warrants further exploration.

Our data suggest that SYN115 may be abrogating adenosine signaling in the tumor microenvironment, thereby favoring the Tpex-to-Tex transition. While this may be favorable in the short-term, it may deplete the Tpex compartment necessary for the long-term antitumor immune response, explaining the lack of clinical relevance of targeting the adenosine signaling pathway that we observe in our preclinical model.

In recent years, systemic cancer therapies have been proposed that aim to inhibit the enzymatic activity of CD73 or adenosine signaling through A2AR.[19-21,37] These therapies are often combined with other treatments, such as anti-PD-1 therapy, to achieve a more significant benefit, typically through a synergistic effect.[19-21] Our results suggest that the immunological consequences of targeting the CD73–adenosine axis may be more nuanced than a purely "relief from immunosuppression" model, because CD73 and A2AR signaling can influence exhaustion dynamics through potentially distinct mechanisms and at different stages of chronic activation. Accordingly, a concern raised by our findings is that some CD73-targeting antibodies could, in principle, engage non-enzymatic signaling and thereby modulate exhaustion trajectories, an idea that warrants direct mechanistic and efficacy-oriented testing in future work.

Interestingly, we observed that CD73-deficient OT-I cells transcriptionally resembled Tpex and presented a competitive advantage over OT-I lymphocytes *in vivo*, observing higher frequencies of OT-I/CD73KO cells in DLN and tumor. In this line, previous work from our laboratory demonstrated that transferring antigen-specific CD73-deficient OT-I cells was more effective in reducing tumor burden in B16.OVA melanoma-bearing mice and resulted in lower expression of PD-1, LAG-3, and CD39 than observed with OT-I cells.[36] This work also demonstrated that CD73 restricts the metabolic fitness and Tc1 differentiation of CD8+ T lymphocytes *in vitro*.[36] Building on these observations, future studies could test whether engineering adoptively transferred CD8$^+$ T cells (or CAR T cells) lacking CD73, or otherwise

modulating this pathway in a cell-intrinsic manner, improves persistence and functional durability in chronic antigen contexts. Likewise, our SYN115 results support the broader caution that system-level depletion of A2AR signaling may shift exhaustion trajectories toward more terminal phenotypes under certain conditions, highlighting the importance of defining treatment window, combination context, and cell-type specificity when evaluating adenosinergic interventions.

Disclosure of potential conflicts of interest

The authors declare no conflict of interest.

Funding

This work was supported by Centro Científico y Tecnológico de Excelencia Ciencia & Vida, FB210008, FB2100082 from Agencia Nacional de Investigación y Desarrollo ANID (DS, MR, AL, MRB), ANID FONDECYT grants 1220196 (DS), 1230183 (MRB), 1212070 (AL), 32207413, 3220741 (AHO), ANID PhD grants: 21201553 (JSA), 21230809 (CB), PhD scholarship grant Fundación María Ghilardi Venegas (SG), ANID Master grants 22221673 (MGG), 22241251 (FM) and CONICYT/FONDEQUIP EQM220027 (DS) and EQM140016 (MRB), EQM1400164.

Author contributions

CRediT: **Juan Saavedra-Almarza:** Conceptualization, Formal analysis, Investigation, Methodology, Visualization, Writing – original draft, Writing – review & editing; **Solange Gouët:** Formal analysis, Investigation, Methodology, Writing – review & editing; **Felipe Malgue:** Investigation; **Catalina Bascuñan:** Formal analysis, Investigation, Writing – original draft; **Andrés Hernández-Oliveras:** Investigation, Writing – original draft; **Joaquín De la Rosa:** Investigation, Methodology; **Javiera Reyes-Alvarez:** Investigation; **Camilo Villaman:** Formal analysis, Investigation; **José Corrales-Bermúdez:** Investigation, Methodology; **Justine Castañeda:** Investigation; **Moira García-Gómez:** Formal analysis, Investigation; **Alberto J.M. Martin:** Conceptualization, Methodology, Software; **Álvaro Lladser:** Conceptualization, Writing – review & editing; **Mario Rosemblatt:** Conceptualization, Project administration, Supervision; **María Rosa Bono:** Conceptualization, Project administration, Resources, Supervision, Writing – review & editing; **Daniela Sauma:** Conceptualization, Funding acquisition, Project administration, Resources, Supervision, Validation, Visualization, Writing – original draft, Writing – review & editing.

ORCID

Álvaro Lladser 0000-0002-5576-1478
Daniela Sauma 0000-0001-8622-3245

Data availability statement

The data obtained from the RNAseq analysis (Fastq files and raw count data) have been deposited at Gene Expression Omnibus (accession code GSE298159). Data are available upon reasonable request from the lead contact, Daniela Sauma (dsauma@uchile.cl).

Ethics approval

All the animal experiments were conducted in accordance with the ARRIVE guidelines and approved by the Institutional Animal Care and Use Committee (CICUA) of Universidad de Chile (Protocol 2211-FCS-UCH).

Generative AI statement

While preparing this work, the authors used ChatGPT and Grammarly to improve the readability and language flow of the manuscript. After using this tool/service, the authors reviewed and edited the content as needed and take complete responsibility for the publication's content.

Limitations of this study

We acknowledge the limitations of the B16.OVA melanoma model in representing the complexities of endogenous, polyclonal antitumor $CD8^+$ T-cell responses. The artificial nature of this model may impact the generalizability of our

findings. Specifically, we recognize that this system relies on a monoclonal T-cell population, which may not reflect the diverse T-cell repertoire found in natural tumor environments. Additionally, the model's reliance on a specific antigen can limit its applicability to tumors with heterogeneous antigen expression. We also acknowledge the limitations of our *in vitro* exhaustion model as a mechanistic discovery tool rather than a full replication of the tumor microenvironment. In addition, although our data is suggestive that CD73 accelerates Tpex-to-Tex differentiation through a nonenzymatic, costimulatory function, further studies are needed to fully demonstrate the costimulatory function of CD73 in our setting. Relatedly, our inference from KO-versus-APCP comparisons is necessarily indirect, because we did not quantify AMP hydrolysis under the exact time/dose conditions used here; therefore, incomplete enzymatic blockade cannot be fully excluded in this specific setting. Finally, our *in vivo* SYN115 experiment should be interpreted as a system-level perturbation of A2AR signaling, since the antagonist is administered systemically and A2AR is expressed across multiple immune and stromal compartments; thus, these *in vivo* results do not by themselves establish a $CD8^+$ T-cell-intrinsic mechanism and should be integrated with our genetic A2ARKO evidence.

References

1. Gebhardt T, Park SL, Parish IA. Stem-like exhausted and memory CD8(+) T cells in cancer. Nat Rev Cancer. 2023;23(11):780–98. doi: 10.1038/s41568-023-00615-0.
2. Khan O, Giles JR, McDonald S, Manne S, Ngiow SF, Patel KP, Werner MT, Huang AC, Alexander KA, Wu JE, et al. TOX transcriptionally and epigenetically programs CD8(+) T cell exhaustion. Nature. 2019;571(7764):211–8. doi: 10.1038/s41586-019-1325-x.
3. Scott AC, Dündar F, Zumbo P, Chandran SS, Klebanoff CA, Shakiba M, Trivedi P, Menocal L, Appleby H, Camara S, et al. TOX is a critical regulator of tumour-specific T cell differentiation. Nature. 2019;571(7764):270–4. doi: 10.1038/s41586-019-1324-y.
4. Kallies A, Zehn D, Utzschneider DT. Precursor exhausted T cells: key to successful immunotherapy? Nat Rev Immunol. 2020;20(2):128–36. doi: 10.1038/s41577-019-0223-7.
5. Miller BC, Sen DR, Al Abosy R, Bi K, Virkud YV, LaFleur MW, Yates KB, Lako A, Felt K, Naik GS, et al. Subsets of exhausted CD8(+) T cells differentially mediate tumor control and respond to checkpoint blockade. Nat Immunol. 2019;20(3):326–36. doi: 10.1038/s41590-019-0312-6.
6. Siddiqui I, Schaeuble K, Chennupati V, Fuertes Marraco SA, Calderon-Copete S, Pais Ferreira D, Carmona SJ, Scarpellino L, Gfeller D, Pradervand S, et al. Intratumoral Tcf1(+)PD-1(+)CD8(+) T cells with stem-like properties promote tumor control in response to vaccination and checkpoint blockade immunotherapy. Immunity. 2019;50(1):195–211.e10. doi: 10.1016/j.immuni.2018.12.021.
7. Brummelman J, Mazza EMC, Alvisi G, Colombo FS, Grilli A, Mikulak J, Mavilio D, Alloisio M, Ferrari F, Lopci E, et al. High-dimensional single cell analysis identifies stem-like cytotoxic CD8(+) T cells infiltrating human tumors. J Exp Med. 2018;215(10):2520–35. doi: 10.1084/jem.20180684.
8. Jansen CS, Prokhnevska N, Master VA, Sanda MG, Carlisle JW, Bilen MA, Cardenas M, Wilkinson S, Lake R, Sowalsky AG, et al. An intra-tumoral niche maintains and differentiates stem-like CD8 T cells. Nature. 2019;576(7787):465–70. doi: 10.1038/s41586-019-1836-5.
9. Sade-Feldman M, Yizhak K, Bjorgaard SL, Ray JP, de Boer CG, Jenkins RW, Lieb DJ, Chen JH, Frederick DT, Barzily-Rokni M, et al. Defining T cell states associated with response to checkpoint immunotherapy in melanoma. Cell. 2018;175(4):998–1013.e20. doi: 10.1016/j.cell.2018.10.038.
10. Franco F, Jaccard A, Romero P, Yu YR, Ho PC. Metabolic and epigenetic regulation of T-cell exhaustion. Nat Metab. 2020;2(10):1001–12. doi: 10.1038/s42255-020-00280-9.
11. Gupta PK, Godec J, Wolski D, Adland E, Yates K, Pauken KE, Cosgrove C, Ledderose C, Junger WG, Robson SC, et al. CD39 expression identifies terminally exhausted CD8+ T cells. PLoS Pathog. 2015;11(10):e1005177. doi: 10.1371/journal.ppat.1005177.
12. Martinez-Usatorre A, Carmona SJ, Godfroid C, Yacoub Maroun C, Labiano S, Romero P. Enhanced phenotype definition for precision isolation of precursor exhausted tumor-infiltrating CD8 T cells. Front Immunol. 2020;11:340. doi: 10.3389/fimmu.2020.00340.
13. Vijayan D, Young A, Teng MWL, Smyth MJ. Targeting immunosuppressive adenosine in cancer. Nat Rev Cancer. 2017;17(12):709–24. doi: 10.1038/nrc.2017.86.
14. Mastelic-Gavillet B, Navarro Rodrigo B, Décombaz L, Wang H, Ercolano G, Ahmed R, Lozano LE, Ianaro A, Derré L, Valerio M, et al. Adenosine mediates functional and metabolic suppression of peripheral and tumor-infiltrating CD8(+) T cells. J Immunother Cancer. 2019;7(1):257. doi: 10.1186/s40425-019-0719-5.
15. Bono MR, Fernández D, Flores-Santibáñez F, Rosemblatt M, Sauma D. CD73 and CD39 ectonucleotidases in T cell differentiation: beyond immunosuppression. FEBS Lett. 2015;589(22):3454–60. doi: 10.1016/j.febslet.2015.07.027.
16. Gabriel SS, Tsui C, Chisanga D, Weber F, Llano-León M, Gubser PM, Bartholin L, Souza-Fonseca-Guimaraes F, Huntington ND, Shi W, et al. Transforming growth factor-β-regulated mTOR activity preserves cellular metabolism to maintain long-term T cell responses in chronic infection. Immunity. 2021;54(8):1698–714e5. doi: 10.1016/j.immuni.2021.06.007.

17. Boison D, Yegutkin GG. Adenosine metabolism: emerging concepts for cancer therapy. Cancer Cell. 2019;36(6):582–96. doi: 10.1016/j.ccell.2019.10.007.
18. Willingham SB, Hotson AN, Miller RA. Targeting the A2AR in cancer; early lessons from the clinic. Curr Opin Pharmacol. 2020;53:126–33. doi: 10.1016/j.coph.2020.08.003.
19. Allard B, Pommey S, Smyth MJ, Stagg J. Targeting CD73 enhances the antitumor activity of anti-PD-1 and anti-CTLA-4 mAbs. Clin Cancer Res. 2013;19(20):5626–35. doi: 10.1158/1078-0432.CCR-13-0545.
20. Beavis PA, Milenkovski N, Henderson MA, John LB, Allard B, Loi S, Kershaw MH, Stagg J, Darcy PK. Adenosine receptor 2A blockade increases the efficacy of Anti-PD-1 through enhanced antitumor T-cell responses. Cancer Immunol Res. 2015;3(5):506–17. doi: 10.1158/2326-6066.CIR-14-0211.
21. Myojin Y, McCallen JD, Ma C, Bauer KC, Ruf B, Benmebarek MR, Green BL, Wabitsch S, McVey JC, Fu C, et al. Adenosine A2a receptor inhibition increases the anti-tumor efficacy of anti-PD1 treatment in murine hepatobiliary cancers. JHEP Rep. 2024;6(1):100959. doi: 10.1016/j.jhepr.2023.100959.
22. Cekic C, Linden J. Adenosine A2A receptors intrinsically regulate CD8+ T cells in the tumor microenvironment. Cancer Res. 2014;74(24):7239–49. doi: 10.1158/0008-5472.CAN-13-3581.
23. Flores-Santibáñez F, Fernández D, Meza D, Tejón G, Vargas L, Varela-Nallar L, Flores-Santibáñez F, Varela-Nallar L, Arredondo S, Guixé V, et al. CD73-mediated adenosine production promotes stem cell-like properties in mouse Tc17 cells. Immunology. 2015;146(4):582–94. doi: 10.1111/imm.12529.
24. Todd KL, Lai J, Sek K, Huang YK, Newman DM, Derrick EB, Koay H, Nguyen D, Hoang TX, Petley EV, et al. A(2A)R eGFP reporter mouse enables elucidation of A(2A)R expression dynamics during anti-tumor immune responses. Nat Commun. 2023;14(1):6990. doi: 10.1038/s41467-023-42734-0.
25. Wang X, Zhang T, Song Z, Li L, Zhang X, Liu J, Qiu L, Qian Z, Zhou S, Feng L, et al. Tumor CD73/A2aR adenosine immunosuppressive axis and tumor-infiltrating lymphocytes in diffuse large B-cell lymphoma: correlations with clinicopathological characteristics and clinical outcome. Int J Cancer. 2019;145(5):1414–22. doi: 10.1002/ijc.32144.
26. Zhang T, Liu H, Jiao L, Zhang Z, He J, Li L, Qiu L, Qian Z, Zhou S, Gong W, et al. Genetic characteristics involving the PD-1/PD-L1/L2 and CD73/A2aR axes and the immunosuppressive microenvironment in DLBCL. J Immunother Cancer. 2022;10(4):e004114. doi: 10.1136/jitc-2021-004114.
27. Dianzani U, Redoglia V, Bragardo M, Attisano C, Bianchi A, Di Franco D, Ramenghi U, Wolff H, Thompson LF, Pileri A, et al. Co-stimulatory signal delivered by CD73 molecule to human CD45RAhiCD45ROlo (naive) CD8+ T lymphocytes. J Immunol. 1993;151(8):3961–70. doi: 10.4049/jimmunol.151.8.3961.
28. Gutensohn W, Resta R, Misumi Y, Ikehara Y, Thompson LF. Ecto-5'-nucleotidase activity is not required for T cell activation through CD73. Cell Immunol. 1995;161(2):213–7. doi: 10.1006/cimm.1995.1029.
29. Massaia M, Perrin L, Bianchi A, Ruedi J, Attisano C, Altieri D, Rijkers GT, Thompson LF. Human T cell activation. Synergy between CD73 (ecto-5'-nucleotidase) and signals delivered through CD3 and CD2 molecules. J Immunol. 1990;145(6):1664–74. doi: 10.4049/jimmunol.145.6.1664.
30. Resta R, Hooker SW, Laurent AB, Shuck JK, Misumi Y, Ikehara Y, Koretzky GA, Thompson LF. Glycosyl phosphatidylinositol membrane anchor is not required for T cell activation through CD73. J Immunol. 1994;153(3):1046–53. doi: 10.4049/jimmunol.153.3.1046.
31. Resta R, Thompson LF. T cell signalling through CD73. Cell Signal. 1997;9(2):131–9. doi: 10.1016/S0898-6568(96)00132-5.
32. Resta R, Yamashita Y, Thompson LF. Ecto-enzyme and signaling functions of lymphocyte CD73. Immunol Rev. 1998;161:95–109. doi: 10.1111/j.1600-065X.1998.tb01574.x.
33. Thompson LF, Ruedi JM. Functional characterization of ecto-5'-nucleotidase-positive and -negative human T lymphocytes. J Immunol. 1989;142(5):1518–22. doi: 10.4049/jimmunol.142.5.1518.
34. Thompson LF, Ruedi JM, Glass A, Low MG, Lucas AH. Antibodies to 5'-nucleotidase (CD73), a glycosyl-phosphatidylinositol-anchored protein, cause human peripheral blood T cells to proliferate. J Immunol. 1989;143(6):1815–21. doi: 10.4049/jimmunol.143.6.1815.
35. Yamashita Y, Hooker SW, Jiang H, Laurent AB, Resta R, Khare K, Coe A, Kincade PW, Thompson LF. CD73 expression and fyn-dependent signaling on murine lymphocytes. Eur J Immunol. 1998;28(10):2981–90. doi: 10.1002/(SICI)1521-4141(199810)28:10<2981::AID-IMMU2981>3.0.CO;2-D.
36. Briceño P, Rivas-Yañez E, Rosemblatt MV, Parra-Tello B, Farías P, Vargas L, Simon V, Cárdenas C, Lladser A, Salazar-Onfray F, et al. CD73 ectonucleotidase restrains CD8+ T cell metabolic fitness and anti-tumoral activity. Front Cell Dev Biol. 2021;9:638037. doi: 10.3389/fcell.2021.638037.
37. Deng WW, Li YC, Ma SR, Mao L, Yu GT, Bu LL, Kulkarni AB, Zhang W, Sun Z. Specific blockade CD73 alters the "exhausted" phenotype of T cells in head and neck squamous cell carcinoma. Int J Cancer. 2018;143(6):1494–504. doi: 10.1002/ijc.31534.
38. Zhao M, Kiernan CH, Stairiker CJ, Hope JL, Leon LG, van Meurs M, Brouwers-Haspels I, Boers R, Gribnau J, van IJcken WFJ, et al. Rapid in vitro generation of bona fide exhausted CD8+ T cells is accompanied by Tcf7 promotor methylation. PLoS Pathog. 2020;16(6):e1008555. doi: 10.1371/journal.ppat.1008555.
39. Fagerberg E, Attanasio J, Dien C, Singh J, Kessler EA, Abdullah L, Shen J, Hunt BG, Connolly KA, De Brouwer E, et al. KLF2 maintains lineage fidelity and suppresses CD8 T cell exhaustion during acute LCMV infection. Science. 2025;387(6735):eadn2337. doi: 10.1126/science.adn2337.

40. McCutcheon SR, Swartz AM, Brown MC, Barrera A, McRoberts Amador C, Siklenka K, Humayun L, ter Weele MA, Isaacs JM, Reddy TE, et al. Transcriptional and epigenetic regulators of human CD8. Nat Genet. 2023;55(12):2211–23. doi: 10.1038/s41588-023-01554-0.
41. Davis LN, Walker ZJ, Reiman LT, Parzych SE, Stevens BM, Jordan CT, Forsberg PA, Sherbenou DW. MYC inhibition potentiates CD8+ T cells against multiple myeloma and overcomes immunomodulatory drug resistance. Clin Cancer Res. 2024;30(14):3023–35. doi: 10.1158/1078-0432.CCR-24-0256.
42. Toumi R, Deo R, Bhise S, Sarkar S, Kalia V. Exploring the role of c-Myc in defining the fate of exhausted CD8 T cells. J Immunol. 2022;208(1_Supplement):182.32–182.32. doi: 10.4049/jimmunol.208.Supp.182.32.
43. Chen S, Fan J, Xie P, Ahn J, Fernandez M, Billingham LK, Miska J, Wu JD, Wainwright DA, Fang D, et al. CD8+ T cells sustain antitumor response by mediating crosstalk between adenosine A2A receptor and glutathione/GPX4. J Clin Invest. 2024;134(8):e170071. doi: 10.1172/JCI170071. PMID: 38441967; PMCID: PMC11014673.
44. Odorizzi PM, Pauken KE, Paley MA, Sharpe A, Wherry EJ. Genetic absence of PD-1 promotes accumulation of terminally differentiated exhausted CD8+ T cells. J Exp Med. 2015;212(7):1125–37. doi: 10.1084/jem.20142237.
45. Huang AC, Postow MA, Orlowski RJ, Mick R, Bengsch B, Manne S, Xu W, Harmon S, Giles JR, Wenz B, et al. T-cell invigoration to tumour burden ratio associated with anti-PD-1 response. Nature. 2017;545(7652):60–65. doi: 10.1038/nature22079. Epub 2017 Apr 10. PMID: 28397821; PMCID: PMC5554367.